THE JOURNAL OF PHYSICAL CHEMISTRY B

Article

pubs.acs.org/JPCB

Effective and Reversible DNA Condensation Induced by a Simple Cyclic/Rigid Polyamine Containing Carbonyl Moiety

Chao Li,[†] Chunying Ma,[†] Pengxiang Xu,[§] Yuxing Gao,[§] Jin Zhang,[†] Renzhong Qiao,*[,†,‡] and Yufen Zhao[§]

[†]State Key Laboratory of Chemical Resource Engineering, Beijing University of Chemical Technology, Beijing, 100029, P. R. China

[‡]State Key Laboratory of Natural and Biomimetic Drugs School of Pharmaceutical Sciences, Peking University Health Science Center, Beijing, 100191, P. R. China

[§]Department of Chemistry, College of Chemistry and Chemical Engineering, Xiamen University, Xiamen 361005, P. R. China

Supporting Information

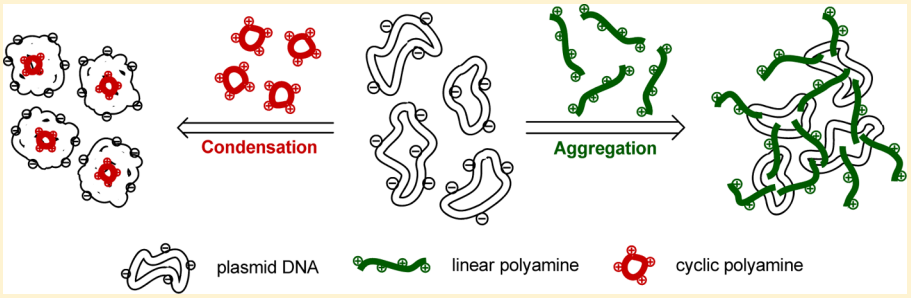

ABSTRACT: The transfection of DNA in gene therapy largely depends on the possibility of obtaining its condensation. The details of nanoparticle formation are essential for functioning, as mediated by the diverse elements containing molecular structure, ionic strength in mediums, and condensing motivator. Here, we report two kinds of DNA condensing agents based on simple cyclic/rigid polyamine molecules, having evaluated their structural effect on nanoparticle formation. The reversible condensation−dissociation process was achieved by ion-switching, attributing to a possible condensing mechanism—competitive building of external hydrogen bonds. Using poly[$(dA\text{-}dT)_2$] and poly[$(dG\text{-}dC)_2$] as substrates, respectively, circular dichroism (CD) signals clearly presented dissimilar interactions between polyamines and both rich sequences, implying potential preference for G−C sequence. The presence of divalent ion Zn^{2+} as an efficient motivator accelerated the achievement of DNA condensation, and an accessible schematic model was depicted to explain the promotion in detail. In addition, by comparison with the behaviors of linear polyamines, differences between condensation and aggregation were explicitly elucidated in aspects of morphology and surface charges, as well as induced condition. The present work may have the potential to reveal the precise mechanism of DNA nanoparticle formation and, in particular, be applied to gene delivery as an efficient nonviral vector.

INTRODUCTION

DNA condensation by simple artificial molecules or large biomolecules has been extensively studied due to its importance in gene therapy, biotechnology, and bionanotechnology.[1−10] Morphologically, DNA compaction may happen either as a monomolecular condensation[11,12] or as a multimolecular aggregation.[13,14] Further, condensation refers to compaction of finite size and of an orderly morphology as compared to aggregation, which can be better used for the purpose of gene delivery due to well-defined small particles.[15,16] A wide variety of multivalent cations, including polyamines, inorganic salts and complexes, dehydrating solvents and cationic lipids, can provoke DNA nanoparticle formation.[17−22] Over the last two decades, natural or synthetic polyamines have attracted more attention as vital and ubiquitous cellular components supporting the structure, conformation, and function of nucleic acids and proteins, as well as maintaining cellular homeostasis.[23] Also, for some low-molecular-weight polyamines, water solubility and full protonation at physiological pH impart unique functional characteristics in their ability to interact with biological macromolecules.

Recently, we reported that two simple cyclic and rigid polyamines could efficiently induce plasmid DNA to form nanoparticles at high temperature.[24] The ultimate size of globules formed was little enough to gain higher electrophoresis mobility than that for any plasmid forms (supercoiled, relaxed, or linear). However, a large percentage of previous studies on polyamines, such as spermine/spermidine, dendrimer, and Thomas' synthetic polyamines, showed a complete gel retardation phenomenon as one of condensed evidence. Two distinct results suggested that cyclic/rigid polyamine/DNA polyplexes could be much denser than those polyplexes in gel loading well, largely resulting from different molecular structures and mechanisms. Although a possible mechanism

Received: December 27, 2012
Revised: May 10, 2013

   dx.doi.org/10.1021/jp312766u | J. Phys. Chem. B XXXX, XXX, XXX−XXX

Scheme 1. The Structures of Cyclic/Rigid Polyamine Analogues and the Basic Structural Unit

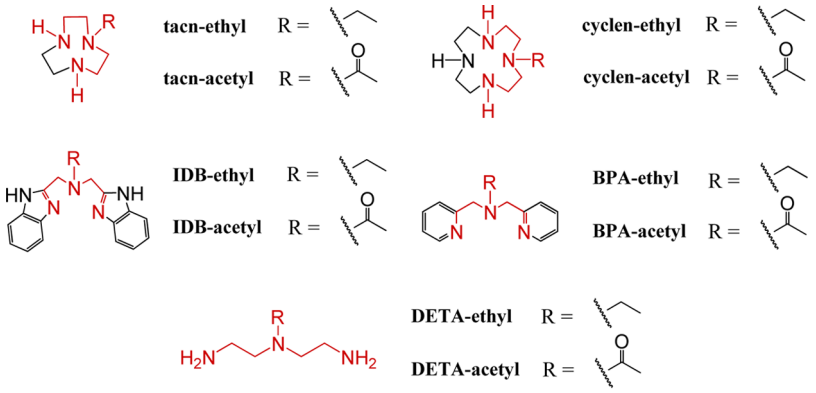

was proposed in our previous study, detailed evidence and discussion behind these significative phenomena were scant. Thus, it is imperative to systematically investigate the intricacies of DNA condensation using cyclic/rigid polyamine and to reveal a reasonable mechanism of interaction between small molecules and biomacromolecules, as well as to compare functions of various polyamines in the condensing process.

In the work presented here, we therefore constructed several cyclic/rigid polyamine-based analogues and evaluated the structural effect on extent and size of plasmid DNA condensation. Importantly, ionic strength could mediate condensation−dissociation switching, referring to competitive building of external hydrogen bonds as a possible mechanism. On the basis of the assumption above, we also found a potential preference for G−C sequences by the evidence of CD spectra. In addition, comparative studies concerning morphology and surface charges were performed in the presence of typical linear polyamines including spermidine and spermine, which further clarified different molecular structural effects on particular condensing features.

MATERIALS AND METHODS

Materials. MS (ESI) mass spectral data were recorded on a Finnigan LCQDECA mass spectrometer. ^{1}H NMR and ^{13}C NMR spectra were measured on a Bruker AV600 spectrometer, and chemical shifts in ppm were reported relative to internal Me_4Si ($CDCl_3$). All other chemicals and reagents were obtained commercially and used without further purification. Electrophoresis grade agarose, plasmid DNA (pUC18), poly-[(dA-dT)$_2$], and poly[(dG-dC)$_2$] were purchased from Promega Corporation. Calf thymus DNA (CT DNA) was purchased from Sigma (USA) Company and used as received. Each polyamine−Zn^{2+} solution is a mixture of Zn^{2+} and polyamine with the same molar concentration.

Gel Electrophoresis Assay. Electrophoresis experiments were performed with plasmid DNA (pUC18). In a typical experiment, supercoiled pUC18 DNA (5 μL, 0.05 $\mu g{\cdot}\mu L^{-1}$) in Tris−HCl buffer (40 mM, pH 7.4) was treated with different concentration catalyst, followed by dilution with Tris−HCl buffer to a total volume of 80 μL. The samples were then incubated at different temperature and time, and loaded on a 1% agarose gel containing 1.0 $\mu g{\cdot}mL^{-1}$ ethidium bromide (EB). The electrophoresis apparatus consisted of a Biomeans Stack II-Electrophoresis system, PPSV-010. Electrophoresis was carried out at 85 V for 1 h in TAE buffer, and bands were visualized by UV light and photographed, recorded on an Olympus Grab-IT2.0 Annotating Image Computer System.

AFM Assay. Atomic force microscope (AFM) imaging was performed in tapping mode on a Digital Instruments multimode NanoScope III having a maximal lateral range of approximately 5 μm. All images were analyzed by tapping in air.

High-quality mica sheets (FluorMica) were cut with scissors into squares (1 cm × 1 cm) and attached with superglue to 15 mm round stainless steel sample disks (Ted Pella). Before each use, the mica was freshly cleaved by pulling off the top sheets with tape and then covered with 10 μL of autoclaved AFM buffer (10 mM Tris pH 7.5, 1 mM EDTA, 5 mM $MgCl_2$). The surface was precoated with Mg^{2+} to allow negatively charged DNA to bind. After 5 min, the buffer was rinsed thoroughly with 0.5 mL of distilled water, and the mica was briefly dried under a stream of N_2 (g).

The DNA sample was diluted with AFM buffer to 2.5 $ng{\cdot}\mu L^{-1}$, and then, 10 μL of diluted sample was dropwise added to the mica surface. After 5 min, the buffer was rinsed thoroughly with 0.5 mL of distilled water, and the mica was briefly dried under a stream of N_2 (g). Each sample was scanned independently three times, and three different areas were chosen in each scan.

Particle Size and Zeta-Potential Measurements. The polyplexes were prepared at varying N/P (polyamine/phosphate) ratios from 0/1 to 24/1 by adding a solution of polyamines (2 μL, varying concentrations) to a solution of plasmid DNA (8 μL, 15 $ng{\cdot}\mu L^{-1}$), followed by vortexing for 5 s and incubating at 50 °C for 6 h. The surface charge and the size of polyplexes were measured at 25 °C with a Zetasizer Nano ZS instrument (Malvern) equipped with a standard capillary electrophoresis cell and dynamic light scattering (DLS, 10 mW He−Ne laser, 633 nm wavelength), respectively. The measurements were performed in triplicate.

CD Experiments. Circular dichroism (CD) experiments were performed under a continuous flow of nitrogen using a Jasco-810 spectropolarimeter. A path length cell of 1 cm was used, and all experiments were performed at room temperature. A 0.5 μM solution of polyamine molecule was titrated into the 60 $\mu g{\cdot}mL^{-1}$ DNA solutions (at pH 7.4, 10 mM Tris−HCl buffer with 10 mM NaCl). The standard scan parameters for all experiments used a wavelength range from 400 to 220 nm. Sensitivity was set at 100 mdeg and a scan speed of 200 nm/min. Three scans were made and computer averaged.

dx.doi.org/10.1021/jp312766u | J. Phys. Chem. B XXXX, XXX, XXX−XXX

RESULTS

Design and Synthesis of Polyamines. Previous work showed that cyclen-acetyl and IDB-acetyl were excellent agents for DNA condensation in aqueous solution.[24] Carbonyl in molecules, as an unintentional modification, potentially contributed to external hydrogen bonds building between DNA bases and condensing agents, and was considered as a key factor in nanoparticle formation. For this reason, we here synthesized a series of control polyamines modified by an ethyl or acetyl side chain, including 1,4,7,10-tetraazacyclododecane (cyclen), 1,4,7-triazacyclononane (tacn), bis(2-benzimidazolylmethyl)amine (IDB), and bis(2-pyridylmethyl)-amine (BPA). Further, to explore the minimum active group, the common portion (diethylenetriamine, DETA) in these analogues as a basic structural unit was constructed. The studied compounds were shown in Scheme 1, and their synthetic routes were depicted in Scheme S1 of the Supporting Information.

Structural Effect on DNA Condensation. *Condensing Ability.* The EC_{50} value (concentration for 50% of maximal effect) is a good indicator of the efficacy in inducing DNA condensation.[25−27] The real condensed abilities of various analogues studied, however, were hardly presented by comparing EC_{50} values due to their diverse maximal effect. Here, efficacy in condensing DNA was determined by contents (%) of nanoparticles in gel electrophoresis assay under the same conditions. Table 1 shows the contents of condensates induced by different polyamine analogues (2.0 mM) at 50 °C incubation for 8 h with Zn^{2+} or not. Using the acetyl modification, each polyamine analogue presented an excellent ability to condense DNA. Both cyclic polyamines, tacn and cyclen, induced 87.3 and 92.4% plasmid to form nanoparticles in the presence of Zn^{2+}, respectively. The content of condensates induced by rigid structural polyamines seems lower than those of cyclic ones, with 78.9% for IDB and 66.2% for BPA. In the case of the ethyl modification, however, the condensing ability of every candidate sharply decreased, compared with the corresponding acetyl-modified group. The most effective molecule, IDB-ethyl-Zn^{2+}, can induce only 17.3% DNA to form nanoparticles. It could be concluded that achievement of condensation involves oxygen atoms in carbonyl moieties as H-bond acceptor based on an "external hydrogen bond building" mechanism. Thus, ethyl-substituted polyamines have a low ability to condense DNA to nanoparticles whether Zn^{2+} was present. Subsequently, DETA as the basic structural unit was picked to evaluate, but hardly any detectable DNA condensate was obtained in spite of the modification of carbonyl group, suggesting integrated polyamines with intensive charges may provide more opportunities for DNA condensation while the stretched structural DETA with dispersed charges was unable to. In addition, Zn^{2+} involvement dramatically enhanced condensing efficiency, and delicate experiments and statements were shown below.

Table 1. Effect of Polyamines on pUC18 Plasmid DNA Condensation and Diameters of Nanoparticles

	condensates (%)		
polyamine	with Zn^{2+}	without Zn^{2+}	hydrodynamic radius (Rh) (nm) (PDI)
tacn-acetyl	87.3	25.5	67.5 (0.20)
cyclen-acetyl	92.4	25.0	63.9 (0.17)
IDB-acetyl	78.9	17.4	61.2 (0.25)
BPA-acetyl	66.2	13.3	71.6 (0.33)
DETA-acetyl	<1	<1	*a*
tacn-ethyl	11.1	9.7	77.6 (0.35)
cyclen-ethyl	13.0	11.1	69.1 (0.31)
IDB-ethyl	17.3	12.3	73.8 (0.44)
BPA-ethyl	3.5	2.9	88.9 (0.53)
DETA-ethyl	<1	<1	*a*

[a]No valid value was observed.

Size of Condensates. We next determined the diffusion coefficients of polyamine analogues induced DNA condensation using dynamic laser light scattering (DLS), and hydrodynamic radii were calculated using the Stokes−Einstein equation. DLS indicated the presence of compact particles, with hydrodynamic radii ranging from 60 to 90 nm at 25 °C in the presence of different polyamines (Table 1). The acetyl-modified group produced nanoparticles in the range 60−70 nm which were slightly smaller than those corresponding analogues with the ethyl-modified group. Carbonyl in molecules as a potential bonding moiety may supply a strong affinity to further condense. The hydrodynamic radius of polyamines/DNA condensates appeared to be independent of polyamine concentration, while the amount of nanoparticles depended on the concentration used. It was also noteworthy that hydrodynamic radii of nanoparticles measured by DLS were larger than the size estimated from AFM. This was mainly due to the process involved in the preparation of sample. AFM images depicted the size in the dried state of sample, whereas DLS determined the size in the hydrated state.

Effects of Ionic Strength on Reversible Process. *Condensation.* Effect of ions in medium on the formation of DNA nanoparticles was investigated, and the results showed that ionic strength as an effective approach can be used to modulate DNA condensation and dissociation. The transitions of condensation were determined for diverse salt concentration containing 0, 1, 10, 50, and 100 mM sodium chloride, and the content of condensates (%) was plotted against incubated temperature (Figure 1). The plots were sigmoidal with the increase of temperature under the low salt concentration range studied, while the plots for the higher salt concentrations sharply became flat in the same range of temperature.

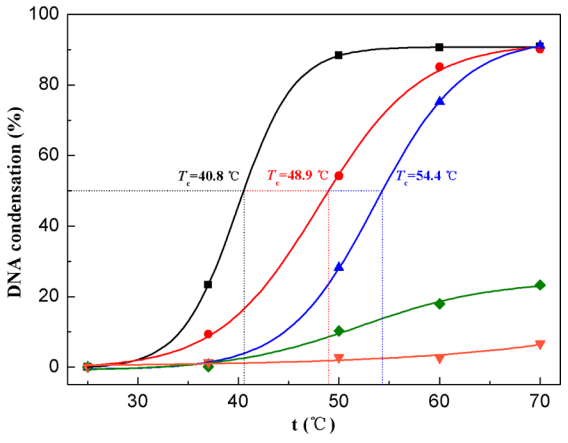

Figure 1. Effect of temperature on pUC18 plasmid DNA condensation under different ionic strength mediums. pUC18 plasmid DNA (0.015 $\mu g \cdot \mu L^{-1}$) was incubated with cyclen-acetyl-Zn^{2+} (2.0 mM) for 8 h. C_{Na^+} = 0 (black ■), C_{Na^+} = 1 mM (red ●), C_{Na^+} = 10 mM (blue ▲), C_{Na^+} = 50 mM (green ◆), C_{Na^+} = 100 mM (orange ▼).

dx.doi.org/10.1021/jp312766u | J. Phys. Chem. B XXXX, XXX, XXX−XXX

As shown in Figure 1, the condensing temperature of polyamines required for DNA nanoparticle formation increased with salt concentration. The efficacy of polyamine analogues in inducing DNA condensation was determined by using the T_c value (the condensing temperature at which 50% of supercoiled DNA is compacted to globules). Without extra ions introduced in the medium, the T_c value of pUC18 DNA was 40.8 °C in the presence of cyclen-acetyl-Zn^{2+}. In the 1 and 10 mM Na^+ buffer, the T_c values were 48.9 and 54.4 °C, respectively. It was difficult for DNA to compact to nanoparticles in the medium containing higher salt concentrations. Only 20 and 5% of the DNA nanoparticles formed in 50 and 100 mM Na^+ buffer, respectively, and no meaningful T_c was depicted.

The findings above suggested that to obtain equivalent condensates in high salt medium required a much higher temperature than that in low ionic strength medium; i.e., high ionic concentration made it harder for DNA condensing. It resembled the correlation between DNA melting (T_m) profiles and ionic strength in medium. Much of what we know about the relation is high ionic concentration makes DNA unwinding more difficult. Therefore, we attempted to explore the probable connection between DNA condensing and unwinding. Table 2 showed the corresponding theoretic T_m (see the Supporting Information for the formula) and experimental T_c over the entire ion concentration range studied. Both T_m and T_c rose gradually with increasing ionic strength in the medium, though the meaningful T_c values were not provided under the higher ionic mediums. Given the relationship between ionic strength and T_m, we have reason to believe that DNA unwinding is what the formation of nanoparticles really desires.

Table 2. The Theoretic T_M and Experimental T_c in the Mediums Containing Different Ionic Concentrations

C_{Na^+} (mM)	<1[a]	1	10	20	50	80	100
theoretic T_m (°C)	<52.3	52.3	68.9	73.9	80.5	83.9	85.5
experimental T_c (°C)	40.8	48.9	54.4	57.8	58.3	*b*	*b*

[a]No extra Na^+ was introduced. [b]The trace amounts of condensates were detected under such ionic conditions, so the T_c values obtained from either experiments or formula were meaningless.

Dissociation. It is essential that the efficiency of nonviral gene delivery vehicles, such as polyamines, partly relies on their ability to release DNA upon entering the cell nucleus. It is therefore of interest to determine under which conditions DNA can be released from condensing agents. Fortunately, the present process of condensation was reversible with introduction of ions. Figure 2 showed that the contents of condensates and free DNA were plotted against incubated time under different ionic strength mediums. At C_{Na^+} = 1 mM, both plots were near linear with increase of release time, and about 50% nanoparticles could be dissociated accompanied with recovering of equivalent free DNA. The extent of dissociation could reach up to 80% under the same time in the presence of 10 mM Na^+, while it just took 2 h and half an hour to achieve the same degree of dissociation at the content of 50 and 100 mM Na^+, respectively. Although no data was provided at the Na^+ concentration up to 150 mM, according to the current tendency, it is easy to believe that the polyplexes could be thoroughly dissociated under physiological conditions. It should be pointed out that no extra Na^+ existed in the release system (C_{Na^+} = 0), but still a near 50% decrease of condensates was clearly observed after 5 h of incubation. The result could be attributed to reasonable degradation of DNA nanoparticles during long exposure to metal complexes rather than release similar to those found under definite ionic strength, which was consistent with the stability of free DNA.

The driving force of the dissociation of polyplexes may mainly involve DNA renaturation with increasing ion strength in the medium. It is well-known in the literature that the increase of ionic strength makes it easy for DNA renaturation.

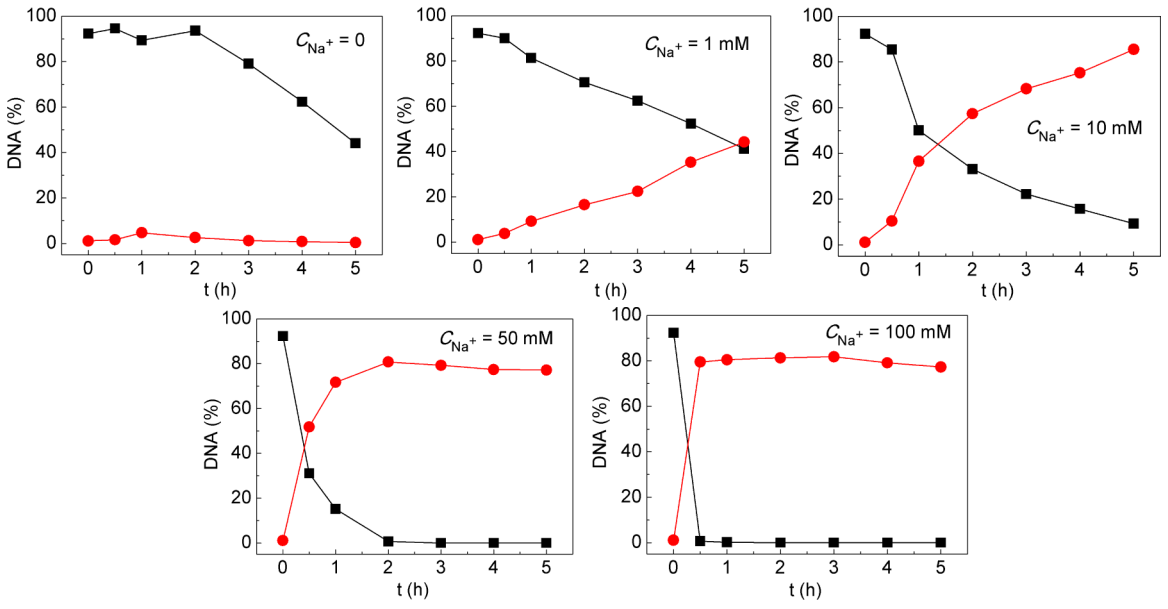

Figure 2. Dissociation of polyamine/pUC18 plasmid DNA polyplexes depending on incubated time under different ionic strengths. The cyclen-acetyl-Zn^{2+} (2.0 mM) condensed pUC18 plasmid DNA (0.015 $\mu g \cdot \mu L^{-1}$) to nanoparticles at 50 °C for 8 h, yielding 90% compacted DNA as substrate. Then, dissociations of these condensates were detected in 5 h at C_{Na^+} = 0, 1, 10, 50, and 100 mM mediums, respectively. Condensates (black ■) and nicked DNA (red ●).

dx.doi.org/10.1021/jp312766u | J. Phys. Chem. B XXXX, XXX, XXX–XXX

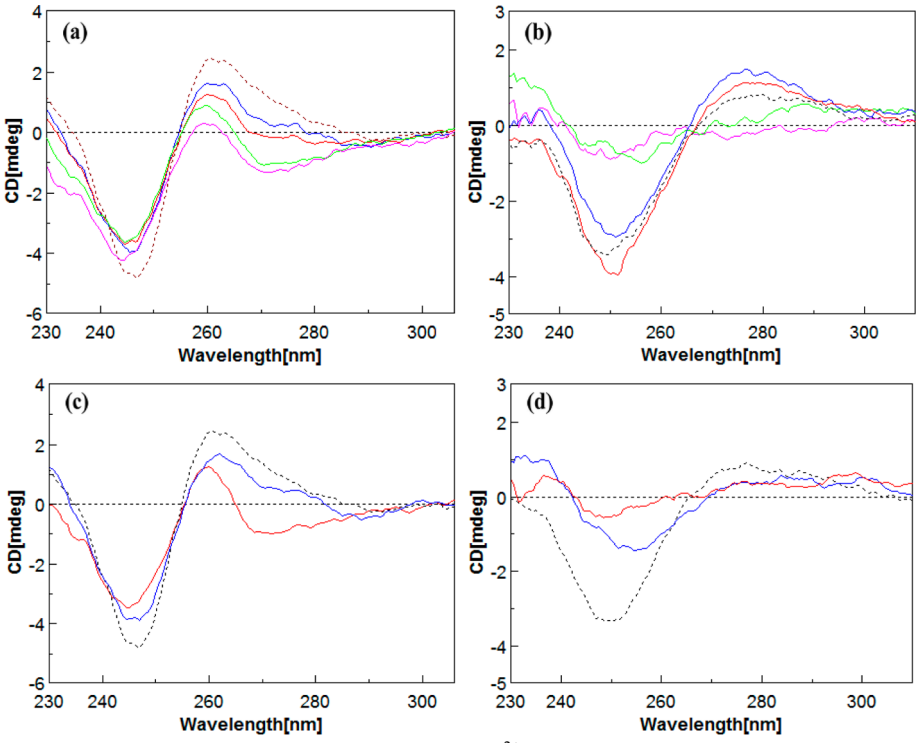

Figure 3. CD spectra of (a) cyclen-acetyl-Zn^{2+}/poly[$(dA\text{-}dT)_2$] and (b) cyclen-acetyl-Zn^{2+}/poly[$(dG\text{-}dC)_2$] at different N/P ratios, 0/1 (dotted line), 1/1 (blue), 2/1 (red), 4/1 (green), and 8/1 (purple). (c) CD spectra for tacn-acetyl-Zn^{2+} (red) or IDB-acetyl-Zn^{2+} (blue)/poly[$(dA\text{-}dT)_2$] and (d) for tacn-acetyl-Zn^{2+} (red) or IDB-acetyl-Zn^{2+} (blue)/poly[$(dG\text{-}dC)_2$] at N/P ratio 8/1.

This is because in a high ionic strength medium the negative charges of phosphate groups in the DNA backbone are neutralized, which resulted in the decrease of electrostatic repulsion among them. Thus, with increase of the ionic strength in the medium, original double strands recover (renaturation), while the formed external hydrogen bonds break rapidly, which could not maintain the compact conformation of condensed DNA, resulting in dissociation of polyplexes. The similar reversible process can be induced by other polyamines, and data of tacn-acetyl-Zn^{2+} and IDB-acetyl-Zn^{2+} are shown in Figure S1 in the Supporting Information.

Sequence Preference in the Condensing Process. Conformational changes of CT-DNA interacting with polyamines were verified by CD experiments, as reported previously;[24] however, more attention focused on whether sequence preference in condensing process existed or not. We here carried out CD experiments on polyamines/poly[$(dG\text{-}dC)_2$] and polyamines/poly[$(dA\text{-}dT)_2$] complexes prepared at different N/P ratios (1/1, 2/1, 4/1, and 8/1), respectively. As a case of cyclen-acetyl-Zn^{2+}, Figure 3a showed the change of CD spectra with the increase of cyclen-acetyl-Zn^{2+}/poly[$(dA\text{-}dT)_2$] ratio. The CD spectrum of uncondensed poly[$(dA\text{-}dT)_2$] showed, as expected, a typical signature (dotted) with a positive peak at 262 nm, a negative peak at 247 nm, and a crossover near 255 nm. Upon the condensation by cyclen-acetyl-Zn^{2+}, a dramatic change in the CD spectra could be observed (blue, red, green, and purple lines), including a significant decreasing both in positive and negative ellipticity and slight blue-shift. Though the shape of the bands was different from the typical ψ-phase,[28−31] decreasing both in positive and negative ellipticity accompanied with blue-shift suggested DNA helices could hardly remain a higher-order chiral structure. The unwinding was likely to occur in the process of condensation. Interestingly, the anomalistic CD spectra were detected in the presence of poly[$(dG\text{-}dC)_2$] as substrate (Figure 3b). The positive ellipticity at 277 nm enhanced slightly when the N/P ratios remained at a low level. At the N/P ratios of 4/1 and 8/1, however, both positive and negative bands were flattened, which were due to a high extent of compaction of complexes. Because losing intensity in both bands suggested a decrease in helicity and denaturation of DNA,[32,33] this could be ascribed to change of DNA conformation or DNA condensation. Compared with the result from cyclen-acetyl-Zn^{2+}/poly[$(dA\text{-}dT)_2$], the stronger variations with respect to the conservative spectrum of B-DNA were observed in the presence of poly[$(dG\text{-}dC)_2$] at the high ratio. Such a difference implied the existence of a strong interaction between agents and poly[$(dG\text{-}dC)_2$], that is, the event of DNA condensation induced by cyclen-acetyl-Zn^{2+} possessed a preference for G−C rich sequences. Three hydrogen bonds existed in each G−C pair, likely resulting in more opportunity to form similar external hydrogen bonds when the partial DNA helices unwinding occurred with the increase of temperature.

In the same way, using tacn-acetyl-Zn^{2+} (red line) and IDB-acetyl-Zn^{2+} (blue line) as candidates, respectively, the similar behaviors of CD signals were detected as shown in Figure 3c and d. Notably, the extent of signal change induced by IDB-acetyl-Zn^{2+} intercalation was smaller than that of tacn-acetyl-Zn^{2+}, and there was no detectable blue-shift, suggesting the void intercalation of rigid IDB molecule after partial DNA unwinding.

Many studies showed that alternative purine−pyrimidine sequences were the only sequences capable of the B ↔ Z transition[34,35] and prone to conformational changes in the presence of condensing agents. To clearly illustrate ligand interaction with different DNA substrates, therefore, we here

dx.doi.org/10.1021/jp312766u | J. Phys. Chem. B XXXX, XXX, XXX−XXX

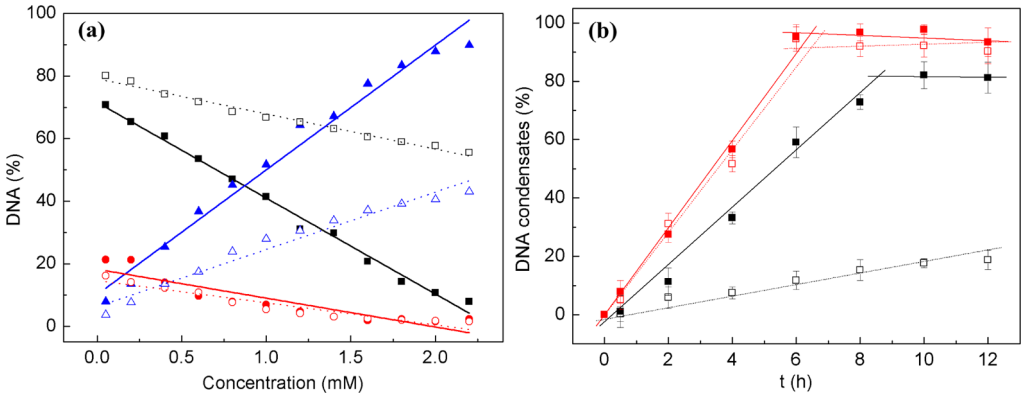

Figure 4. (a) Typical plots of the three plasmid forms against polyamine concentration in the presence and absence of Zn^{2+}. Symbols represent form I DNA with (black ■) and without (black □) Zn^{2+}, form II DNA with (red ●) and without (red ○) Zn^{2+}, and DNA condensates with (blue ▲) and without (blue △) Zn^{2+}. (b) Effect of Zn^{2+} on DNA condensation using form I (black lines) and form II (red lines) as substrates, respectively. Symbols represent cyclen-acetyl (hollow) and cyclen-acetyl-Zn^{2+} (solid).

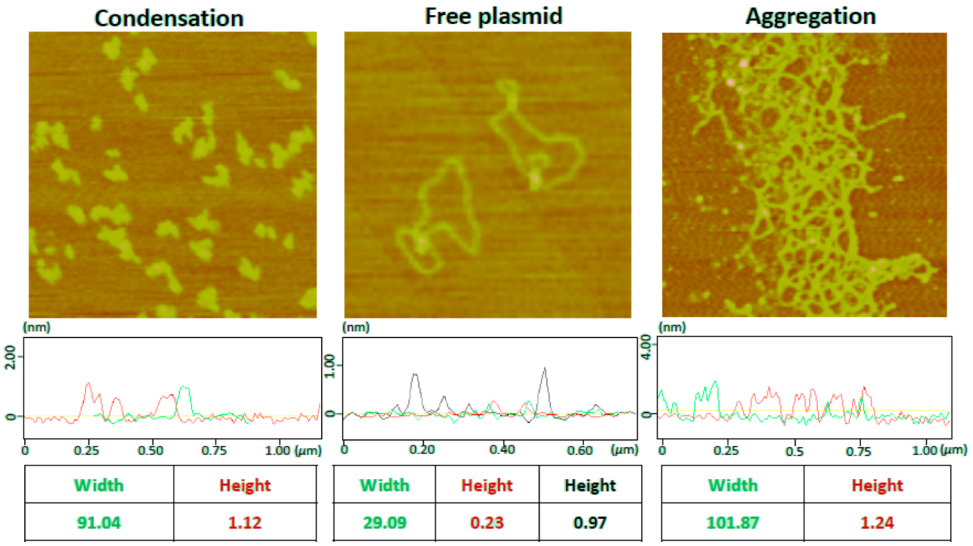

Figure 5. AFM section analysis of pUC18 plasmid DNA, condensates induced by cyclen-acetyl, and aggregates induced by spermine. The scale bar is 100 nm. The height (black) is determined as overlapping.

also chose pUC18 plasmid to evaluate the inducing ability of ligands to DNA conformation, and results were shown in Figure S2 in the Supporting Information.

The CD spectrum of uncondensed pUC18 plasmid DNA exhibited a positive Cotton effect at 273 nm corresponding to base stacking and a negative Cotton effect at 245 nm corresponding to helicity. The CD signals in Figure S2a (Supporting Information) tended to flatten with the increase of cyclen-acetyl-Zn^{2+}/plasmid DNA (N/P) ratio; namely, both positive and negative ellipticity decreased sharply. This suggested a decrease in helicity and denaturation of DNA.[32] At the N/P ratio of 24/1, however, positive ellipticity continued to reduce accompanied with a weak red-shift (from 273 to 278 nm), while the negative part increased promptly, which presented a typical ψ phase as a DNA condensing feature. Meanwhile, the increase of the negative band indicated that the DNA double helix in solution is in a more helical state.[36,37] Similar results were obtained in the IDB-acetyl-Zn^{2+}/pUC18 plasmid DNA protocol, as shown in Figure S2b (Supporting Information).

Compared with the CD signal changes of pUC18 plasmid DNA induced by these condensing agents, the flattening tendency in both bands was more remarkable in the presence of poly[$(dG\text{-}dC)_2$] as substrates. That was because the transition metal ions interacted preferentially with GC sites by chelation to the *N*-7 of guanine and to the phosphate residue,[38] and we believed that ligand in the presence of Zn^{2+} increased the ability of ligand to change the conformation of DNA and to cause DNA condensation.

Promotion of Condensing Rate in the Presence of Zn^{2+}. We also studied the Zn^{2+} effect on the formation of DNA nanoparticles. The previous study showed that polyamines containing Cu^{2+} presented different levels of damage to DNA molecules against potential vectors for gene delivery, thus taking account of toxicity and physiologically relevant reasons, we only focused on Zn^{2+} effects on condensing ability in the current study.

The three plasmid forms (%) were plotted against [cyclen-acetyl] and [cyclen-acetyl-Zn^{2+}], and the results were shown in Figure 4a. The plots were linear for all DNA forms over the entire concentration range studied, but different slopes for the same DNA form were obtained. The plots could be resolved into the decreasing supercoiled (form I, black lines) and the increasing condensates (blue lines), with slope values of −30.6

dx.doi.org/10.1021/jp312766u | J. Phys. Chem. B XXXX, XXX, XXX−XXX

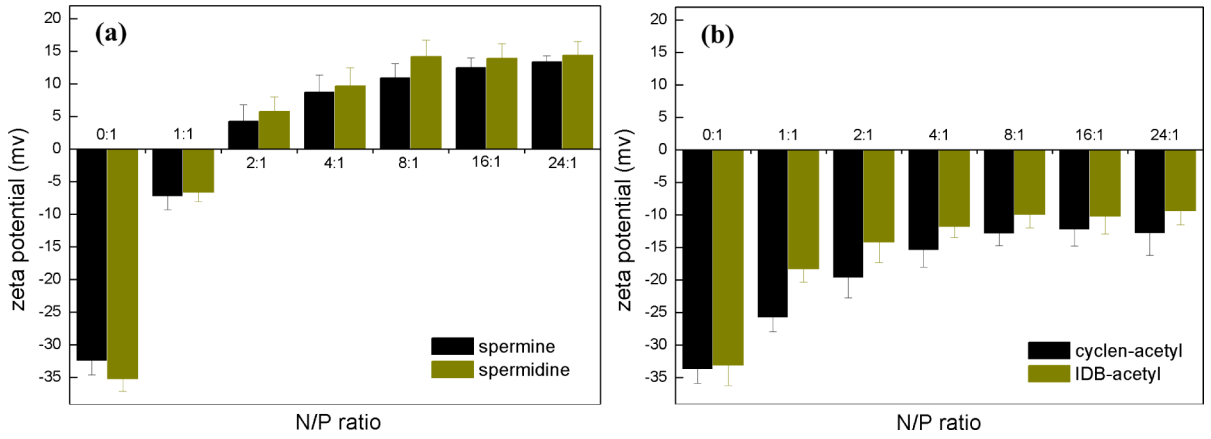

Figure 6. Zeta potential of linear polyamines/pUC18 plasmid DNA (a) and cyclic/rigid polyamines/pUC18 plasmid DNA (b) polyplexes prepared at different N/P ratios ranging from 0/1 to 24/1 at 25 °C for 6 h.

and 39.8 for cyclen-acetyl-Zn^{2+} (solid lines) and −11.2 and 18.3 for cyclen-acetyl (hollow lines). The higher slope values (absolute values) for both form I and condensates indicated that Zn^{2+} could play a positive role in promoting DNA condensation.

Subsequently, we used form I and form II as substrates, respectively, to evaluate the effect of polyamine on condensation, and the contents of condensates were plotted against incubated time (Figure 4b). The plots could be resolved into two linear regions, which indicated that condensation may eventually reach saturation with the increase of time. A higher slope value with Zn^{2+} (black solid) as compared to that of free ligand (black hollow) indicated a faster condensing process in the presence of form I as substrate. In the case of form II, however, both slope values (red lines) were very similar, giving 0.154 h^{-1} with Zn^{2+} and 0.150 h^{-1} without Zn^{2+}, respectively. The results elucidated that the presence of Zn^{2+} can improve the conversion at the stage of "form II → condensate" rather than "form I → condensate". Structurally, open circular DNA (form II) is liable to be compacted to nanoparticles due to its relaxed and loose structure, which exposes more amounts of hydrogen bonds in base pairs for external hydrogen bond formation. Hydrogen bonding interactions between the carbonyl group of polyamines and the H-bond donor of bases are most likely responsible for the accelerated condensing process. It might be necessary to convert form I to form II at the start of condensate formation. Thus, it is believed that promotion of metal ions is derived from conversion of DNA forms.

Comparison between Cyclic/Rigid and Linear Polyamines on DNA Compaction. *Morphology.* The morphological diversity of DNA induced by both linear and cyclic polyamines was clearly presented using AFM section analysis, as shown in Figure 5. The cyclic polyamine can induce plasmid DNA to form nanoparticles as classical globules, with 91.04 nm width and 1.12 nm height. For spermine, however, bulky DNA aggregates were liable to form, because the stretched structure and dispersed charges of linear polyamide may provide more opportunities for cross-linking of DNA. The section analysis presented these aggregates with a width of 101.87 nm and a height of approximately 1.24 nm. The width of double strands in uncompacted DNA was about 29.09 nm, while the height was just 0.23 nm, even 0.97 nm for overlap. Compared with the behavior of linear polyamines, we concluded that condensation could dominate in the process of nanoparticle formation induced by cyclic compounds. Similarly, condensing behaviors of rigid polyamine (IDB-acetyl) and spermidine were investigated, and the results were presented in Figure S3 in the Supporting Information.

Surface Charges. The complexation induced by mixing negatively charged polyelectrolyte DNA and positively charged polyamines was studied by means of zeta potential measurements to detect their surface charges. Figure 6 showed the zeta potential data of cyclic/rigid polyamines/DNA and linear polyamines/DNA complexes at different N/P ratios, respectively. The general trend observed for both experiments was an increase in zeta potential values with the increase in N/P ratios. In the linear polyamine assay (Figure 6a), the zeta potentials increased sharply with charge reverse to positive (−35 mV → 15 mV), indicating aggregates with the positive surface. The increasing of both size and zeta potential value with the increase of linear polyamines/DNA ratio may be explained by progressive growing of clusters formed by the particles around DNA. In contrast, the increase of cyclic/rigid polyamines resulted in only slight enhancement of zeta potential with the negative values from about −35 to −14 mV (Figure 6b), suggesting the surface of condensates completely wrapped with polyanion (DNA). The opposite surface charges of both polyplexes might be derived from different morphologies. The results were consistent with those obtained by electrophoresis and AFM assays.

DISCUSSION

Although DNA condensation containing polyamine analogues has been extensively studied for the past decade, our present efforts attended to the structural effect on formation of nanoparticles from a new perspective. The morphology of polyamines/DNA polyplexes depends on the polyamine type, i.e., cyclic/rigid and linear, from monomolecular condensation for concentrated charges to multimolecular aggregation for dispersive charges. The cyclic/rigid polyamine with carbonyl modification is more efficacious than that with ethyl modification in condensing DNA to nanoparticles, implying the reasonable assumption concerning external hydrogen bonds building during the condensing process.

Generally, preliminary evidence for the ability to induce DNA nanoparticle formation was obtained from a gel retardation assay performed with plasmid DNA, even for small molecular condensing agents. Some similar polyamine

dx.doi.org/10.1021/jp312766u | J. Phys. Chem. B XXXX, XXX, XXX−XXX

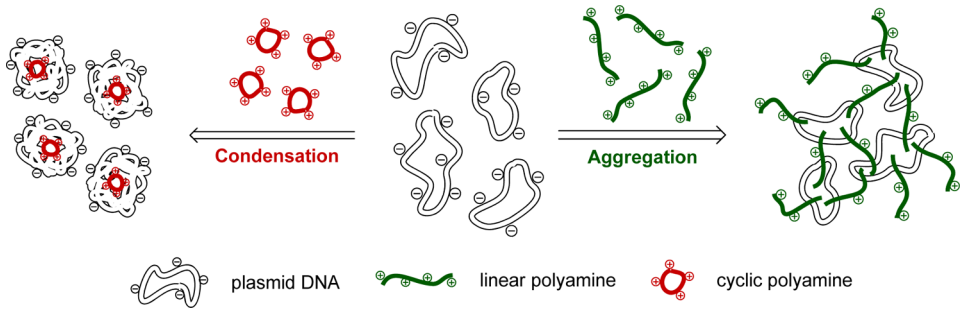

Figure 7. Schematic model to explain the formation of pUC18 plasmid DNA condensation and aggregation.

analogues, reported by Yu et al.[39] and Lu et al.,[40] had the ability to retard plasmid DNA in gel loading well at proper N/P (or charge) ratio. The electrophoretic mobility of DNA was completely inhibited when the diameter of growing polyplexes exceeded the gel pore size. These small molecules as condensing agents hardly wrapped around biomacromolecules carrying positive charges, suggesting the polyplexes in the gel loading well could be cross-linking DNA aggregation rather than condensation of a few DNA molecules. Our present results, however, showed that the DNA condensed by cyclic/rigid polyamines was more mobile during electrophoresis, and possessed a higher electrophoresis mobility than that for any plasmid forms (supercoiled, open circular, and linear). Supposing no mass loss, DNA could be compacted to much smaller particles compared with those being thoroughly retarded, as well as wrapped with negative charges. The volume of polyplexes should be expected to be smaller to overcome membrane across, which is the main barrier toward gene delivery and expression.

The AFM images and reversal of surface charges also clearly elucidated the striking differences of both morphologies. Toroids have been reported to be the most common morphology for DNA complexes,[17] but globules clearly predominate for cyclic/rigid polyamine/DNA polyplexes due to the centralization of positive charges within condensing agents. A schematic model for the formation of condensation and aggregation was depicted in Figure 7. On the basis of the structure of cyclic/rigid polyamine with relatively concentrated amino groups, valid positive charges were restricted within narrow limits. The open circular plasmid shrank and wrapped inward once several positively charged polyamines were placed in it, resulting in appearance of condensation. The zeta potential was negative for all the cyclic/rigid polyamine/DNA ratios increasing from −35 to −14 mV (Figure 6b). On the contrary, when AFM was used to image the mixed sample containing linear polyamine incubated, no monomolecular globule similar to those found in the presence of cyclen-acetyl was observed, but bulky cross-linking aggregation was observed instead. The ability of spermine/spermidine aggregation was related to its linear structure with dispersive charges that make it able to cross-link negatively charged polyelectrolyte such as DNA. Similarly, the Bhattacharya group also successfully constructed two kinds of cholesterol-based lipid derivatives as effective nonviral vectors. The TEM assays presented that the length of spacer in cholesterol-based gemini lipids[41] and molecular weight of PEI in PEI-cholesterol-based lipopolymers[42] played a vital role in morphologies of polyplexes. Most low molecular weight PEI grated cholesterol can induce DNA to form regular spherical complexes, and the gemini cholesterol molecules with short spacers can do likewise. It could be concluded that the centralized structures (or charges) of ligands easily induced DNA to form uniform polyplexes while the dispersive forms (or charges) were apt to generate irregular ones. This conclusion is consistent with our current results about DNA compacting modes mediated by linear/cyclic polyamines.

Charge reversal was clearly observed at an N/P ratio of 2:1, presenting +4.5 mV for spermine and +5.3 mV for spermidine. The same observations have been reported for simple polyamines as well.[43] It is based on an idea that long flexible counterions contacting DNA are not necessarily bound at a stoichiometric equilibrium but may form brushes, etc., and their total charge can be more than the bare DNA charge.

Ionic strength, one of the most critical influences on DNA condensation, was extensively discussed. Static light scattering measured by Thomas et al.[26,44] showed that spermine analogues could trigger λ-DNA condensation, which ability were inhibited with increase of Na^+ concentrations in medium, based on Manning's counterion condensation theory.[45,46] Another study about the influence of salt concentration on condensation was performed by cryo-TEM, indicating that the size of the dendrimer polyamine/DNA polyplex increased when the salt concentration increased.[47] However, we here found that ionic strength had the ability to modulate reversible formation of nanoparticles, that is, the ion-switching of condensation and dissociation. This finding is based on the fact that the reversible process depended on ionic concentration as well as temperature, and achieved by the way of DNA unwinding and renaturation. When DNA was incubated at proper temperature for a long time, original hydrogen bonds between A−T or G−C could become less stable and even break (DNA unwinding). The carbonyl of condensing agents competitively interacted with the H atom in DNA bases, and then new weak hydrogen bonds formed (DNA condensation). However, introduction of Na^+ drove the broken hydrogen bonds retrieved according to the principle of complementary base pairing. The external hydrogen bonds disappeared, and interaction of charge neutralization remained, which could not maintain the compact conformation of condensed DNA, resulting in dissociation (DNA renaturation). There is no contradiction between external hydrogen bonds-driven and Manning's counterion condensation, instead interaction of counterion made DNA and small molecules more close for building of new bonds.

Although some positively charged polyelectrolytes interacted with DNA via electrostatic interactions without sequence specificity, a certain extent of G−C sequence preference of cyclic/rigid polyamine was detected under the current protocol. Unlike the typical ψ-phase of CT-DNA, totally different behaviors of alternating purine-pyrimidine sequence polynu-

dx.doi.org/10.1021/jp312766u | J. Phys. Chem. B XXXX, XXX, XXX−XXX

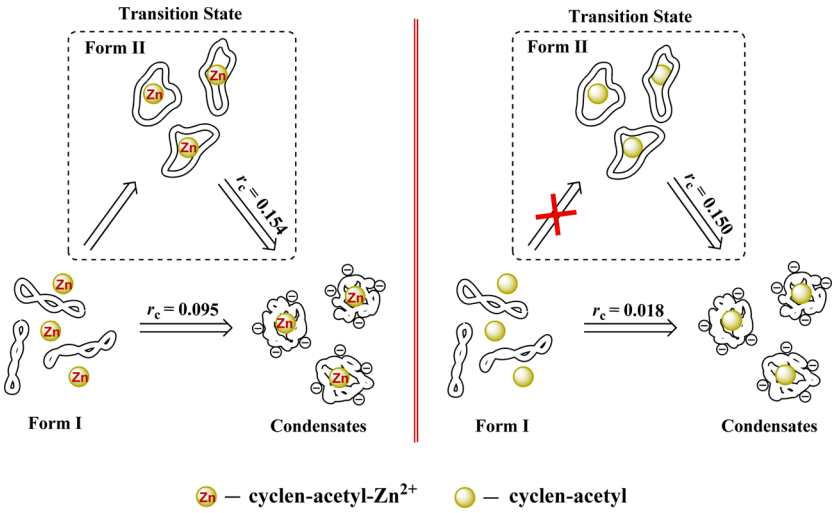

Figure 8. Schematic model to explain the Zn^{2+} effect on pUC18 plasmid DNA condensation based on different substrates. The slope values in Figure 4b were used to represent the approximate rate of condensation (r_c).

cleotides were observed. Flattened ellipticities for poly[(dG-dC)$_2$] as substrate were distinguished from interaction with poly[(dA-dT)$_2$] (Figure 3a,b). The amount of original hydrogen bonds between two kinds of base pairs as well as available bonding heteroatom could lead to a distinct affinity to DNA, causing quite different and discernible CD signal changes. For IDB-acetyl-Zn^{2+}, the intercalation interaction between rigid molecules and DNA may be a key force to drive DNA condensation. Meanwhile, the steric hindrance from two benzimidazole molecules may have a certain influence on affinity to the nucleic acid skeleton, resulting in the weaker signal changes to both rich sequences than that of tacn-acetyl-Zn^{2+} at the same N/P (Figure 3c,d). Nevertheless, external hydrogen bonds building between DNA and condensing molecules were a prerequisite for condensation, because detectable CD signal changes were not found in the system that consisted of ethyl-mediated groups, such as cyclen-ethyl, IDB-ethyl, etc.

As for metal ions in condensing agents, although Liu et al.[48,49] presented tri- and multibenzimidazole metal complexes possessing DNA condensing property, more attention was attracted to form and maintain steady complexes which can bind DNA better by the way of intercalation or electrostatic attraction. Barely any report concerned their effects on the process of condensation. In our case, Zn^{2+} acceleration to condensation could be achieved through "pretreating" plasmid. The different condensing rates from two substrates should be attributed to the presence of transition states. Possible processes of DNA condensation based on different substrates in the presence or absence of Zn^{2+} were depicted as shown in Figure 8. For open circular DNA (form II) as substrate, the existence of Zn^{2+} had almost no promotion to condensation proved by similar r_c, whereas both agents presented the striking diversity on supercoiled plasmid (form I) with r_c = 0.095 for Zn^{2+} complex and r_c = 0.018 for free ligand, respectively. The results suggested the existence of a transition state—form II DNA. Before formation of nanoparticles, form I as substrate was primarily converted to form II, which process could be acceleratedly completed in the presence of complex due to superior cleavage ability. Thus, the "pretreating" of metal complex to supercoiled DNA contributed to more rapid and thorough condensation as compared with the corresponding free ligand.

CONCLUSIONS

In summary, we synthesized a series of cyclic and rigid polyamine analogues as efficient condensing agents based on the previous findings, and an overall study concerning their influence on DNA condensation was performed. Acetyl-modified polyamines were more efficacious than ethyl-modified ones in provoking DNA nanoparticle formation, indicating that original hydrogen bond breaking and external competitive building were the major forces governing DNA nanoparticle formation. On the basis of this mechanism, low ionic strength was liable to realize DNA compacting through DNA double-strand unwinding early, while high Na^+ concentration in medium easily triggered condensate dissociation, suggesting an ion-switching of DNA condensation−dissociation. Besides, we also compared different morphologies and surface charges of two kinds of polyamine, and the results elucidated condensation induced by charge-concentrated cyclic/rigid polyamines and aggregation formed by charge-dispersed linear ones. Detailed investigations into the potential for gene delivery are still ongoing; the present results should be of value for efficient design of small condensing molecules, as well as profound understanding of condensation mechanism.

ASSOCIATED CONTENT

Supporting Information

Detailed synthetic routes and data of all compounds, the formula for the melting temperature of DNA, the dissociation process for tacn-acetyl-Zn^{2+} and IDB-acetyl-Zn^{2+}, the CD assays for pUC18 plasmid DNA, and the AFM section analysis of IDB-acetyl and spermidine. This material is available free of charge via the Internet at http://pubs.acs.org.

AUTHOR INFORMATION

Corresponding Author

*Address: 53 Mailbox, 15, Beisanhuan EastRoad, Chaoyang Distict, Beijing, 100029, P. R. China. Phone: 86 10 64413899. Fax: 86 10 82728926. E-mail: qiao_group@163.com.

dx.doi.org/10.1021/jp312766u | J. Phys. Chem. B XXXX, XXX, XXX−XXX

Author Contributions

C.L. and C.M. performed experiments and calculations. P.X., Y.G., and J.Z. analyzed data. R.Q. and Y.Z. contributed reagents and analytical tools. C.L. wrote the paper.

Notes

The authors declare no competing financial interest.

■ ACKNOWLEDGMENTS

Support of this research by the National Nature Science Foundation of China is gratefully acknowledged (Nos. 20972014, 21202005, 21232005, and 21172016.). We thank Ms Yanxia Jia from Institute of Biophysics, Chinese Academy of Sciences, for AFM.

■ REFERENCES

(1) Qiua, X.; Parsegian, V. A.; Rau, D. C. Divalent Counterion-Induce Condensation of Triple-Strand DNA. *Proc. Natl. Acad. Sci. U.S.A.* **2010**, *107*, 21482−21486.
(2) Ziebarth, J.; Wang, Y. Coarse-Grained Molecular Dynamics Simulations of DNA Condensation by Block Copolymer and Formation of Core-Corona Structures. *J. Phys. Chem. B* **2010**, *114*, 6225−6232.
(3) Liu, Y.; Yu, L.; Chen, Y.; Zhao, Y.-L.; Yang, H. Construction and DNA Condensation of Cyclodextrin-Based Polypseudorotaxanes with Anthryl Grafts. *J. Am. Chem. Soc.* **2007**, *129*, 10656−10657.
(4) Wang, X.-L.; Zhang, X.-H.; Cao, M.; Zheng, H.-Z.; Xiao, B.; Wang, Y.; Li, M. Gemini Surfactant-Induced DNA Condensation into a Beadlike Structure. *J. Phys. Chem. B* **2009**, *113*, 2328−2332.
(5) Froehlich, E.; Mandeville, J. S.; Arnold, D.; Kreplak, L.; Tajmir-Riahi, H. A. PEG and mPEG-Anthracene Induce DNA Condensation and Particle Formation. *J. Phys. Chem. B* **2011**, *115*, 9873−9879.
(6) Haley, J.; Geng, Y. Role of DNA in Condensation and Combinative Self-Assembly. *Chem. Commun. (Cambridge, U. K.)* **2010**, *46*, 955−957.
(7) Wang, Y.; Ran, S.; Man, B.; Yang, G. Ethanol Induces Condensation of Single DNA Molecules. *Soft Matter* **2011**, *7*, 4425−4434.
(8) Kurzbach, D.; Velte, C.; Arnold, P.; Kizilsavas, G.; Hinderberger, D. DNA Condensation with Spermine Dendrimers: Interactions in Solution, Charge Inversion, and Morphology Control. *Soft Matter* **2011**, *7*, 6695−6704.
(9) Meng, X.; Liu, L.; Zhou, C.; Wang, L.; Liu, C. Dinuclear Copper(II) Complexes of a Polybenzimidazole Ligand: Their Structures and Inductive Roles in DNA Condensation. *Inorg. Chem.* **2008**, *47*, 6572−6574.
(10) Lidgi-Guigui, N.; Guis, C.; Brissault, B.; Kichler, A.; Leborgne, C.; Scherman, D.; Labdi, S.; Curmi, P. A. Investigation of DNA Condensing Properties of Amphiphilic Triblock Cationic Polymers by Atomic Force Microscopy. *Langmuir* **2010**, *26*, 17552−17557.
(11) Post, C. B.; Zimm, B. H. Internal Condensation of a Single DNA Molecule. *Biopolymers* **1979**, *18*, 1487−1501.
(12) Widom, J.; Baldwin, R. L. Monomolecular Condensation of λ-DNA Induced by Cobalt Hexammine. *Biopolymers* **1983**, *22*, 1595−1620.
(13) Post, C. B.; Zimm, B. H. Theory of DNA Condensation: Collapse versus Aggregation. *Biopolymers* **1982**, *21*, 2123−2137.
(14) Teif, V. B.; Bohinc, K. Condensed DNA: Condensing the Concepts. *Prog. Biophys. Mol. Biol.* **2011**, *105*, 208−222.
(15) Rao, N. M. Cationic Lipid-Mediated Nucleic Acid Delivery: Beyond Being Cationic. *Chem. Phys. Lipids* **2010**, *163*, 245−252.
(16) Vijayanathan, V.; Thomas, T.; Thomas, T. J. DNA Nanoparticles and Development of DNA Delivery Vehicles for Gene Therapy. *Biochemistry* **2002**, *41*, 14085−14094.
(17) Bloomfield, V. A. DNA Condensation. *Curr. Opin. Struct. Biol.* **1996**, *6*, 334−341.
(18) Bloomfield, V. A. Condensation of DNA by Multivalent Cations: Considerations on Mechanism. *Biopolymer* **1991**, *31*, 1471−1481.
(19) Koltover, I.; Wagner, K.; Safinya, C. R. DNA Condensation in Two Dimensions. *Proc. Natl. Acad. Sci. U.S.A.* **2000**, *97*, 14046−14051.
(20) Brewer, L. R.; Corzett, M.; Balhorn, R. Protamine-Induced Condensation and Decondensation of the Same DNA Molecule. *Science* **1999**, *286*, 120−123.
(21) Munoz-Ubeda, M.; Misra, S. K.; Barran-Berdon, A. L.; Aicart-Ramos, C.; Sierra, M. B.; Biswas, J.; Kondaiah, P.; Junquera, E.; Bhattacharya, S.; Aicart, E. Why Is Less Cationic Lipid Required to Prepare Lipoplexes from Plasmid DNA than Linear DNA in Gene Therapy? *J. Am. Chem. Soc.* **2011**, *133*, 18014−18017.
(22) Bhattacharya, S.; Bajaj, A. Advances in Gene Delivery through Molecular Design of Cationic Lipids. *Chem. Commun. (Cambridge, U. K.)* **2009**, *45*, 4632−4656.
(23) Thomas, T.; Thomas, T. J. Polyamines in Cell Growth and Cell Death: Molecular Mechanisms and Therapeutic Applications. *Cell. Mol. Life Sci.* **2001**, *2*, 244−258.
(24) Li, C.; Tian, H.; Duan, S.; Liu, X.; Xu, P.; Qiao, R.; Zhao, Y. Controllable DNA Condensation-Release Induced by Simple Azaheterocyclic-Based Metal Complexes. *J. Phys. Chem. B* **2011**, *115*, 13350−13354.
(25) Korolev, N.; Zhao, Y.; Allahverdi, A.; Eom, K. D.; Tam, J. P.; Nordenskiold, L. The Effect of Salt on Oligocation-Induced Chromatin Condensation. *Biochem. Biophys. Res. Commun.* **2012**, *418*, 205−210.
(26) Vijayanathan, V.; Lyall, J.; Thomas, T.; Shirahata, A.; Thomas, T. J. Ionic, Structural, and Temperature Effects on DNA Nanoparticles Formed by Natural and Synthetic Polyamines. *Biomacromolecules* **2005**, *6*, 1097−1103.
(27) Nayvelt, I.; Hyvonen, M. T.; Alhonen, L.; Pandya, I.; Thomas, T.; Khomutov, A. R.; Vepsalainen, J.; Patel, R.; Keinanen, T. A.; Thomas, T. J. DNA Condensation by Chiral α-Methylated Polyamine Analogues and Protection of Cellular DNA from Oxidative Damage. *Biomacromolecules* **2010**, *11*, 97−105.
(28) Bombelli, C.; Borocci, S.; Diociaiuti, M.; Galantini, L.; Luciani, P.; Mancini, G.; Sacco, M. G. Role of the Spacer of Cationic Gemini Amphiphiles in the Condensation of DNA. *Langmuir* **2005**, *21*, 10271−10274.
(29) Bombelli, C.; Faggioli, F.; Luciani, P.; Mancini, G.; Sacco, M. G. PEGylated Lipoplexes: Preparation Protocols Affecting DNA Condensation and Cell Transfection Efficiency. *J. Med. Chem.* **2007**, *50*, 6274−6278.
(30) Bombelli, C.; Faggioli, F.; Luciani, P.; Mancini, G.; Sacco, M. G. Efficient Transfection of DNA by Liposomes Formulated with Cationic Gemini Amphiphiles. *J. Med. Chem.* **2005**, *48*, 5378−5382.
(31) Fant, K.; Esbjorner, E. K.; Lincoln, P.; Norden, B. DNA Condensation by PAMAM Dendrimers: Self-Assembly Characteristics and Effect on Transcription. *Biochemistry* **2008**, *47*, 1732−1740.
(32) Clarke, M. J.; Jansen, B.; Marx, K. A.; Kruger, R. Biochemical Effects of Binding $[(H_2O)(NH_3)_5Ru^{II}]^{2+}$ to DNA and Oxidation to $[(NH_3)_5Ru^{III}]_n$—DNA. *Inorg. Chim. Acta* **1986**, *124*, 13−28.
(33) Yang, P.; Wang, H.; Gao, F.; Yang, B. Antitumor Activity of the Cu(II)-Mitoxantrone Complex and Its Interaction with Deoxyribonucleic Acid. *J. Inorg. Biochem.* **1996**, *62*, 137−145.
(34) Pohl, F. M.; Jovin, T. M. Salt-Induced Co-operative Conformational Change of a Synthetic DNA: Equilibrium and Kinetic Studies with Poly(dG-dC). *J. Mol. Biol.* **1972**, *67*, 375−396.
(35) Rich, A.; Nordheim, A.; Wang, A. H. J. The Chemistry and Biology of Left-Handed Z DNA. *Annu. Rev. Biochem.* **1984**, *53*, 791−846.
(36) Zuidam, N. J.; Barenholz, Y.; Minsky, A. Chiral DNA Packaging in DNA-Cationic Liposome Assemblies. *FEBS Lett.* **1999**, *457*, 419−422.
(37) Tanaka, K.; Okahata, Y. A DNA-Lipid Complex in Organic Media and Formation of an Aligned Cast Film. *J. Am. Chem. Soc.* **1996**, *118*, 10679−10683.

(38) Zimmer, C.; Luck, G.; Triebel, H. Conformation and Reactivity of DNA. IV. Base Binding Ability of Transition Metal Ions to Native DNA and Effect on Helix Conformation with Special References to DNA−Zn(II) Complex. *Biopolymers* **1974**, *13*, 425−453.
(39) Zhang, Q.-F.; Yang, W.-H.; Yi, W.-J.; Zhang, J.; Ren, J.; Luo, T.-Y.; Zhu, W.; Yu, X.-Q. 1,4,7-Triazycyclononane-Containing Cationic Lipids with Ester Bond: Preparation and Application in Gene Delivery. *Bioorg. Med. Chem. Lett.* **2011**, *21*, 7045−7049.
(40) Yan, H.; Li, Z.-F.; Guo, Z.-F.; Lu, Z.-L.; Wang, F.; Wu, L.-Z. Effective and Reversible DNA Condensation Induced by Bifunctional Molecules Containing Macrocyclic Polyamines and Naphthyl Moieties. *Bioorg. Med. Chem.* **2012**, *20*, 801−808.
(41) Bajaj, A.; Kondaiah, P.; Bhattacharya, S. Synthesis and Gene Transfer Activities of Novel Serum Compatible Cholesterol-Based Gemini Lipids Possessing Oxyethylene-Type Spacers. *Bioconjugate Chem.* **2007**, *18*, 1537−1546.
(42) Bajaj, A.; Kondaiah, P.; Bhattacharya, S. Synthesis and Gene Transfection Efficacies of PEI-Cholesterol-Based Lipopolymers. *Bioconjugate Chem.* **2008**, *19*, 1640−1651.
(43) Besteman, K.; Van Eijk, K.; Lemay, S. G. Charge Inversion Accompanies DNA Condensation by Multivalent Ions. *Nat. Phys.* **2007**, *3*, 641−644.
(44) Nayvelt, I.; Thomas, T.; Thomas, T. J. Mechanistic Differences in DNA Nanoparticle Formation in the Presence of Oligolysines and Poly-l-lysine. *Biomacromolecules* **2007**, *8*, 477−484.
(45) Manning, G. S. Limiting Laws and Counterion Condensation in Polyelectrolyte Solutions I. Colligative Properties. *J. Chem. Phys.* **1969**, *51*, 924−933.
(46) Manning, G. S.; Ray, J. Counterion Condensation Revisited. *J. Biomol. Struct. Dyn.* **1998**, *16*, 461−476.
(47) Carnerup, A. M.; Ainalem, M.-L.; Alfredsson, V.; Nylander, T. Condensation of DNA Using Poly(amido amine) Dendrimers: Effect of Salt Concentration on Aggregate Morphology. *Soft Matter* **2011**, *7*, 760−768.
(48) Meng, X.; Liu, L.; Zhang, H.; Luo, Y.; Liu, C. Tris-(benzimidazolyl)amine-Cu(II) Coordination Units Bridged by Carboxylates: Structures and DNA-Condensing Property. *Dalton Trans.* **2011**, *40*, 12846−12855.
(49) Liu, L.; Zhang, H.; Meng, X.; Yin, J.; Li, D.; Liu, C. Dinuclear Metal(II) Complexes of Polybenzimidazole Ligands as Carriers for DNA Delivery. *Biomaterials* **2010**, *31*, 1380−1391.